Infrared Matrix Isolation and Theoretical Studies on Glutarimide

D. C. Bieńko,[†] D. Michalska,*[,†] S. Roszak,[‡] and W. Wojciechowski[†]

Institute of Inorganic Chemistry and Institute of Physical and Theoretical Chemistry, Technical University of Wrocław, Wybrzeże Wyspiańskiego 27, 50-370 Wrocław, Poland

M. J. Nowak and L. Lapinski

Institute of Physics, Polish Academy of Science, Al. Lotników 32/46, 02-668 Warsaw, Poland

Received: February 27, 1997; In Final Form: May 30, 1997[⊗]

Infrared spectra of glutarimide isolated in low-temperature Ar and N_2 matrixes are reported. The molecular structure, vibrational frequencies, and infrared intensities of glutarimide are calculated with ab initio Hartree−Fock and second-order Møller−Plesset perturbation (MP2) methods as well as with density functional theory (DFT) using the nonlocal gradient corrected functional (BP86). The best overall agreement between the calculated and experimental spectra has been obtained at the MP2/D95V** level. Unequivocal assignment of the experimental infrared bands is performed on the basis of the potential energy distribution (PED). A striking similarity is noted for frequencies of the corresponding CO and NH vibrations in glutarimide and in uracil, thymine, and their methyl derivatives. Furthermore, the significant flattening of the glutarimide ring, predicted by calculations, indicates its structural resemblance to pyrimidine bases. It is suggested that some glutarimide drugs are able to intercalate between nucleic base pairs in the DNA helix or they may act as antagonists of uracil and thymine in biological processes.

Introduction

Glutarimide, GI (2,6-piperidinedione), is a structural part of a number of molecules with interesting biochemical activity. Several glutarimide derivatives have been reported to possess significant anticancer activity. For example, PCNU [λ-(chloroethyl)-3-(2,6-piperidinedione)-1-nitrosourea] can easily cross the blood−brain barrier, and it shows activity against brain tumors;[1] aminoglutethimide is a strong inhibitor of steroid biogenesis and is used in the treatment of metastatic breast cancer;[2] and antineoplaston A10 (*N*-phenylacetyl-α-aminoglutarimide), which has recently been introduced into experimental chemotherapy, has a remarkable anticancer activity, particularly against brain tumors, and it shows very low toxicity.[3,4] In vitro studies employing the thermal denaturation of DNA as well as fluorescence spectroscopy have revealed that antineoplaston A10 may bind weakly and noncovalently with DNA.[5] Eriguchi et al.[6] suggested that the A10 molecule may enter into DNA since it showed significant chemopreventive effects against various carcinogens in mice.

Glutarimide is also a component of newly synthesized antibiotics which exert antiviral and antifungal activity.[7−9] Cycloheximide, the best known member of glutarimide antibiotics, is a very strong inhibitor of protein synthesis.[10] It has been reported that the biological activity of cycloheximide is due to a specific binding interaction of the glutarimide moiety with a site on the 60 S ribosomal subunit.[11,12] Of particular interest is the fact that replacement of hydrogen in the CO−NH−CO (imide) group with the methyl or acetyl group results in complete loss of activity of glutarimide drugs.[13] This indicates that the biological activity of these drugs is determined by the specific hydrogen bonding between glutarimide and other molecules in biological systems.

Despite the wealth of published papers on pharmacological and biochemical studies on glutarimide drugs, there is very little documented work concerning the structure and vibrational spectra of glutarimide. Recently, Xu and Clark[14] have performed experimental and theoretical studies on the electronic spectra of single crystals of glutarimide. The infrared spectra of glutarimide in solutions have been reported by Thompson et al.;[15] however, the proposed band assignment is very ambiguous.

Knowledge of the molecular structure and vibrational spectra of glutarimide is very important for the investigation of intermolecular interactions using vibrational spectroscopic methods. It is expected that these normal modes of glutarimide which involve vibrations of the imide group should reveal substantial changes in frequency due to the formation of hydrogen bonding with other molecules. Therefore, a clear understanding of the vibrational spectrum of a bare glutarimide is indispensable for a correct assignment of the spectra of hydrogen-bonded systems.

In this work we report, for the first time, the infrared spectra of monomeric glutarimide, measured in low-temperature argon and nitrogen matrixes. Extensive calculations of the structure and infrared spectra of glutarimide have been performed at three theory levels: ab initio Hartree−Fock, MP2, and density functional (DFT).

To get detailed information on the nature of normal modes, the potential energy distributions (PEDs) were calculated at each theory level. These combined spectroscopic and theoretical investigations allowed us to obtain unequivocal and complete vibrational assignment of the infrared spectrum of glutarimide. It is hoped that these results will be helpful for further studies on interaction of glutarimide drugs with biological molecules and may shed some light on the possible mechanism of the biological activity of glutarimide.

Experimental Section

Glutarimide (Aldrich) was purified by vacuum sublimation prior to the matrix experiment. The matrix gases, argon (Linde AG) and nitrogen (Technische Gase, Leipzig), were of purity grade 6.0. The method of matrix preparation and the apparatus

* Author for correspondence.
[†] Institute of Inorganic Chemistry.
[‡] Institute of Physical and Theoretical Chemistry.
[⊗] Abstract published in *Advance ACS Abstracts,* September 15, 1997.

S1089-5639(97)00726-3 CCC: $14.00

were the same as described elsewhere.[16] The sample was placed in the microoven in the vacuum chamber of a continuous-flow liquid helium cryostat. The vapors of the sample coming out from the heated microoven were mixed with the matrix gas, Ar or N_2 (precooled in a liquid nitrogen trap), and deposited on a CsI window on the coldfinger (10 K) of the cryostat. Glutarimide diluted in the matrix gas was deposited until the absorbance of the most intense carbonyl band was close to 1. The matrix gas/dopant ratio was experimentally adjusted to ensure that only the bands due to the monomer were recorded. The concentration of glutarimide in the matrix was sufficiently low that no bands due to associated species (known from the studies with more concentrated matrixes) were observed. The temperature of the cold window was maintained at 10 K. Such a low temperature prevented any diffusion and association during the matrix formation. No sign of thermal decomposition was observed during the experiment. The infrared spectra were recorded on a Perkin-Elmer Model 580B grating spectrophotometer operating at a resolution 1−3 cm^{-1}. Integral intensities of the absorption bands were measured by numerical integration.

Theoretical Methods and Computational Details

All calculations have been carried out using the Gaussian 94 code[17] running on a Cray J916 (XMP) supercomputer. The geometry optimizations and calculations of the vibrational spectra of glutarimide have been performed with ab initio Hartree−Fock (HF) and second-order Møller−Plesset perturbation (MP2) methods (using the frozen core approximation)[18] as well as with density functional theory (DFT).[19] The basis set contained the Huzinaga's (9s5p) primitive set,[20] contracted to the valence double-ζ collection, according to the scheme proposed by Dunning and Hay.[21] The basis set was augmented with a set of six-component d Gaussian polarization functions for heavy atoms and p polarization functions for hydrogen atoms, proposed by Hariharan and Pople.[22] This basis set, denoted as D95V**, has been successfully used in previous calculations of vibrational spectra for molecules of a similar size.[23,24] The above choice of basis set leads to 155 molecular orbitals for glutarimide.

The DFT studies of glutarimide were performed employing three energy functionals: BP86 (Becke's exchange with Perdew correlation functionals),[25,26] BLYP (Becke−Lee−Yang−Parr),[25,27] and B3LYP (the combination of the Becke's three-parameter hybrid exchange functional[28,29] with the LYP correlation functional). The results obtained applying these functionals are comparable. The B3LYP functional tends to overestimate all frequencies. The BP86 results turned out to be the most accurate and quite similar to those obtained with the MP2 calculations, especially for C═O stretching modes and in the low-frequency region. Thus, the BP86 results have been listed in Table 2.

For each level of theory the geometry optimization of glutarimide was performed assuming C_s symmetry (with the symmetry plane passing through N_3, H_{15}, C_6, H_{13}, and H_{14} atoms). The atom numbering is shown in Scheme 1, and the optimized geometry parameters are compared in Table 1. The harmonic vibrational frequencies and eigenvectors as well as the infrared intensities were subsequently calculated using the analytical second derivatives for ab initio methods and numerical differentiation of analytical gradients in the DFT method. To express the normal modes in a molecule-fixed coordinate system, the nonredundant set of internal coordinates was defined as recommended by Fogarasi and Pulay.[30] These coordinates are listed in Table 2. Then the force constant matrices obtained in Cartesian coordinates at each theory level were transformed to internal coordinates, which allowed us to perform normal coordinate analysis, as described in ref 31. The potential energy distributions (PEDs)[32] were calculated using our own program, which follows the formulas for PED matrix elements, given in ref 33. Perhaps the most important information obtained from PED calculations is the extent of mixing of various vibrations (expressed in percent contribution of internal coordinates to the normal mode). This allowed us to make a detailed description of the nature of the observed infrared bands.

TABLE 1: Geometry (Bond Lengths in Angstroms, Angles in Degrees) and the Dipole Moment of Glutarimide Calculated within Hartree−Fock, DFT (BP86 Functional), and MP2 Approaches. Experimental Data Are from the X-ray Crystal Structure of Glutarimide (Ref 38)

parameter[a]	HF	BP86	MP2	exptl[b]
C_1–C_2	1.513	1.526	1.516	1.508, 1.502
C_1–C_6	1.527	1.540	1.530	1.510, 1.486
C_2–N_3	1.384	1.408	1.400	1.391, 1.387
C_2–O_7	1.195	1.231	1.228	1.224, 1.215
N_3–H_{15}	1.002	1.029	1.017	0.88
C_1–H_{10}	1.082	1.102	1.092	0.98
C_1–H_{12}	1.088	1.108	1.097	1.103
C_6–H_{13}	1.087	1.105	1.095	1.11
C_6–H_{14}	1.084	1.104	1.094	0.95
C_1–C_2–N_3	116.2	115.3	115.3	116.9, 116.1
C_2–N_3–C_4	128.2	129.0	128.7	126.9
C_6–C_1–C_2	112.5	113.0	112.1	113.7, 114.0
C_1–C_6–C_5	110.2	110.6	109.9	111.8
O_7–C_2–C_1	123.4	124.3	124.3	123.8, 124.0
H_{15}–N_3–C_2	115.9	115.5	115.6	114.1
C_1–C_2–C_4–C_5	0.0	0.0	0.0	
O_7–C_2–C_1–C_5	179.0	178.7	178.8	
N_3–C_2–C_1–C_5	0.2	0.5	0.7	
H_{15}–N_3–C_2–C_1	178.9	179.2	179.0	
DH[c]	132.6	133.0	130.3	130.2
μ[d]	3.95	3.37	4.21	

[a] The atom numbering is shown in Scheme 1. The calculated structure has C_s symmetry with the mirror plane passing through N_3, H_{15}, C_6, H_{13}, and H_{14} atoms. [b] Due to H-bonding in the crystalline glutarimide, the structure of a molecule is significantly distorted and the corresponding bond lengths and angles on the left and right side of the ring have different experimental values. [c] DH is the dihedral angle between the plane defined by $C_1C_6C_5$ atoms and the plane defined by $C_1C_2C_4C_5$ atoms. [d] Dipole moment in debyes.

The calculated frequencies of all normal modes within the HF method were scaled down by 0.90. For MP2 calculations we have used the factor of 0.96 for all normal modes, except for the modes Q_1−Q_7, which were scaled by 0.935 for the following reason: it is known that frequencies of the N−H, C−H, and O−H stretching vibrations calculated with both HF and MP2 methods are considerably overestimated when compared with the experiment.[24,34−36] This indicates that the harmonic approximation in ab initio calculations is unable to reproduce experimental stretching frequencies for these highly anharmonic vibrations. This problem cannot be resolved by a uniform scaling of all calculated vibrational frequencies since these modes are more anharmonic than the others. Therefore, we have introduced a new scaling factor of 0.935 for the MP2 calculated frequencies of N−H and C−H stretching modes to account for their large anharmonicity. The scaling factor was obtained by a least-squares fit to the infrared and Raman frequencies of N−H and C−H stretches observed for glutarimide and related molecules.[24,34−36]

Results and Discussion

A. Geometry. The optimized geometrical parameters and the experimental data from the single-crystal X-ray analysis of glutarimide[38] are listed in Table 1. The calculated data correspond to a molecule of C_s symmetry in the gas phase.

TABLE 2: Internal Coordinates Used in the Normal-Mode Analysis of Glutarimide (Atom Numbering as in Scheme 1)

definition[a]	Description	Symbol
$S_1=r_{1,2}+r_{5,4}$	$\nu(C_2C_1)+\nu(C_4C_5)$	$\nu^s(C_xC_y)$
$S_2=r_{1,2}-r_{5,4}$	$\nu(C_2C_1)-\nu(C_4C_5)$	$\nu^a(C_xC_y)$
$S_3=r_{2,3}+r_{4,3}$	$\nu(C_2N)+\nu(C_4N)$	$\nu^s(C_xN)$
$S_4=r_{2,3}-r_{4,3}$	$\nu(C_2N)-\nu(C_4N)$	$\nu^a(C_xN)$
$S_5=r_{1,6}+r_{5,6}$	$\nu(C_1C_6)+\nu(C_5C_6)$	$\nu^s(C_yC_z)$
$S_6=r_{1,6}-r_{5,6}$	$\nu(C_1C_6)-\nu(C_5C_6)$	$\nu^a(C_yC_z)$
$S_7=r_{2,7}+r_{4,8}$	$\nu(C_2O_7)+\nu(C_4O_8)$	$\nu^s(C_xO)$
$S_8=r_{2,7}-r_{4,8}$	$\nu(C_2O_7)-\nu(C_4O_8)$	$\nu^a(C_xO)$
$S_9=r_{3,15}$	$\nu(N_3H_{15})$	ν(NH)
$S_{10}=r_{1,10}+r_{5,9}$	$\nu(C_1H_{10})+\nu(C_5H_9)$	ν_1^s CH_2; (C_y)
$S_{11}=r_{1,10}-r_{5,9}$	$\nu(C_1H_{10})-\nu(C_5H_9)$	ν_1^a CH_2; (C_y)
$S_{12}=r_{1,12}+r_{5,11}$	$\nu(C_1H_{12})+\nu(C_5H_{11})$	ν_2^s CH_2; (C_y)
$S_{13}=r_{1,12}-r_{5,11}$	$\nu(C_1H_{12})-\nu(C_5H_{11})$	ν_2^s CH_2; (C_y)
$S_{14}=r_{6,13}+r_{6,14}$	$\nu(C_6H_{13})+\nu(C_6H_{14})$	ν^s CH_2; (C_z)
$S_{15}=r_{6.13}-r_{6,14}$	$\nu(C_6H_{13})-\nu(C_6H_{14})$	ν^a CH_2; (C_z)
$S_{16}=\beta_{3,5,4}-\beta_{2,4,3}+\beta_{1,3,2}-\beta_{6,2,1}+\beta_{5,1,6}-\beta_{6,4,5}$	ring def I	$\beta(R_1)$
$S_{17}=2\beta_{2,4,3}-\beta_{1,3,2}-\beta_{6,2,1}+2\beta_{1,5,6}-\beta_{6,4,5}-\beta_{3,5,4}$	ring def II	$\beta(R_2)$
$S_{18}=\beta_{1,3,2}-\beta_{6,2,1}+\beta_{6,4,5}-\beta_{3,5,4}$	ring def III	$\beta(R_3)$
$S_{19}=\beta_{4,15,3}-\beta_{2,15,3}$	$\beta(N_3H)$	β(NH)
$S_{20}=\beta_{3,7,2}-\beta_{1,7,2}+\beta_{3,8,4}-\beta_{5,8,4}$	$\beta(C_2O_7)+\beta(C_4O_8)$	$\beta^s(C_xO)$
$S_{21}=\beta_{3,7,2}-\beta_{1,7,2}-\beta_{3,8,4}+\beta_{5,8,4}$	$\beta(C_2O_7)-\beta(C_4O_8)$	$\beta^a(C_xO)$
$S_{22}=\beta_{13,14,6}$	sciss C_6HH	sciss CH_2; (C_z)
$S_{23}=\beta_{10,12,1}+\beta_{9,11,5}$	sciss C_yHH (in-phase)	sciss $^sCH_2$; (C_y)
$S_{24}=\beta_{10,12,1}-\beta_{9,11,5}$	sciss C_yHH (out-of-phase)	sciss $^aCH_2$; (C_y)
$S_{25}=\beta_{5,13,6}-\beta_{5,14,6}+\beta_{1,13,6}-\beta_{1,14,6}$	rock C_6HH	rock CH_2; (C_z)
$S_{26}=\beta_{5,13,6}+\beta_{5,14,6}-\beta_{1,13,6}-\beta_{1,14,6}$	wag C_6HH	wag CH_2; (C_z)
$S_{27}=\beta_{5,13,6}-\beta_{5,14,6}-\beta_{1,13,6}+\beta_{1,14,6}$	twist C_6HH	twist CH_2; (C_z)
$S_{28}=A_1-A_2+A_3-A_4+A_5-A_6+A_7-A_8$		rock^s CH_2; (C_y)
$S_{29}=A_1-A_2+A_3-A_4-A_5+A_6-A_7+A_8$		rock^a CH_2; (C_y)
$S_{30}=A_1+A_2-A_3-A_4+A_5+A_6-A_7-A_8$		wag^s CH_2; (C_y)
$S_{31}=A_1+A_2-A_3-A_4-A_5-A_6+A_7+A_8$		wag^a CH_2; (C_y)
$S_{32}=A_1-A_2-A_3+A_4+A_5-A_6-A_7+A_8$		twist^s CH_2; (C_y)
$S_{33}=A_1-A_2-A_3+A_4-A_5+A_6+A_7-A_8$		twist^a CH_2; (C_y)
$S_{34}=\gamma_{15,4,3,2}$	$\gamma(N_3H)$	(NH)
$S_{35}=\gamma_{8,5,4,3}+\gamma_{7,3,2,1}$	$(C_2O_7)+(C_4O_8)$	$\gamma^s(C_xO)$
$S_{36}=\gamma_{8,5,4,3}-\gamma_{7,3,2,1}$	$(C_2O_7)-(C_4O_8)$	$\gamma^a(C_xO)$
$S_{37}=\tau_{4,3,2,1}-\tau_{3,2,1,6}+\tau_{2,1,6,5}-\tau_{1,6,5,4}+\tau_{6,5,4,3}-\tau_{5,4,3,2}$		$\tau(R_1)$
$S_{38}=\tau_{4,3,2,1}-\tau_{2,1,6,5}+\tau_{1,6,5,4}-\tau_{5,4,3,2}$		$\tau(R_2)$
$S_{39}=2\tau_{3,2,1,6}-\tau_{4,3,2,1}-\tau_{2,1,6,5}+2\tau_{6,5,4,3}-\tau_{1,6,5,4}-\tau_{5,4,3,2}$		$\tau(R_3)$

[a] The normalizing factors are omitted for clarity. $r_{i,j}$, the distance between atoms i and j; $\beta_{i,j,k}$, the angle between vectors $k-i$ and $k-j$; $\gamma_{i,j,k,l}$, the angle between the vector $k-i$ and the plane defined by atoms j,k,l; $\tau_{i,j,k,l}$, the dihedral angle between the plane defined by atoms i,j,k and the plane defined by atoms j,k,l; $A_1=\beta_{6,10,1}$; $A_2=\beta_{6,12,1}$; $A_3=\beta_{2,10,1}$; $A_4=\beta_{2,12,1}$; $A_5=\beta_{6,9,5}$; $A_6=\beta_{6,11,5}$; $A_7=\beta_{4,9,6}$; $A_8=\beta_{4,11,5}$. Abbreviations: a, antisymmetric (out-of-phase); s, symmetric (in-phase) with respect to the plane perpendicular to the molecular plane and passing through N_3, H_{15}, C_6, H_{13}, and H_{14} atoms. ν, stretching; β, in-plane bending; γ, out-of-plane bending; def, deformation; sciss, scissoring; rock, rocking; wag, wagging; twist, twisting; τ, torsion.

SCHEME 1: Atom Numbering in Glutarimide

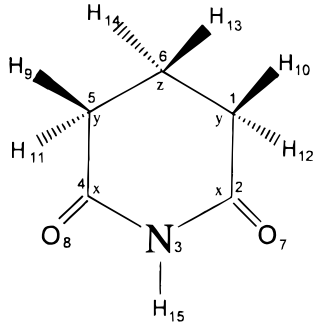

Unfortunately, the experimental gas-phase structure of glutarimide is unknown, whereas the structure of the molecule in the crystal is significantly distorted, due to a strong N−H···O hydrogen bonding, which perturbs the geometry of the ring. Comparison of the calculated and experimental data indicates that the largest discrepancies are encountered for the C−C, C−O, and N−H bond distances. The conformational lability of the ring may affect the experimentally determined C−C bond lengths, as it has been demonstrated in our recent X-ray studies,[39] while the differences in the C−O and N−H bond lengths are understandable, since these bonds are the most susceptible to intermolecular interactions.

The best agreement with the X-ray data has been obtained at the HF level for C−C, C−N, and N−H bond lengths. However, the calculated C═O bond distance is too short, while it is much better predicted with the MP2 method. The BP86 functional considerably overestimates all experimental bond lengths. It should be noted that the calculated bond angles are well reproduced regardless of the theoretical method applied.

It is apparent that the calculated conformation of the molecule may be described as a half-chair, with one carbon atom (C_6) slightly out of the essentially coplanar system, formed by five atoms of the glutarimide ring and two oxygen atoms. The calculated dihedral angle between the $C_1C_6C_5$ plane and the molecular framework is in excellent agreement with the experimental value, as is shown in Table 1. It can be concluded that such significant flattening of the glutarimide ring, predicted by theory and also confirmed by experimental data, enables some glutarimide drugs to intercalate between nucleic base pairs in the DNA helix.

B. Vibrational Spectra. The infrared spectra of glutarimide measured in low-temperature argon and nitrogen matrices are compared with the theoretical spectra in Figure 1. The

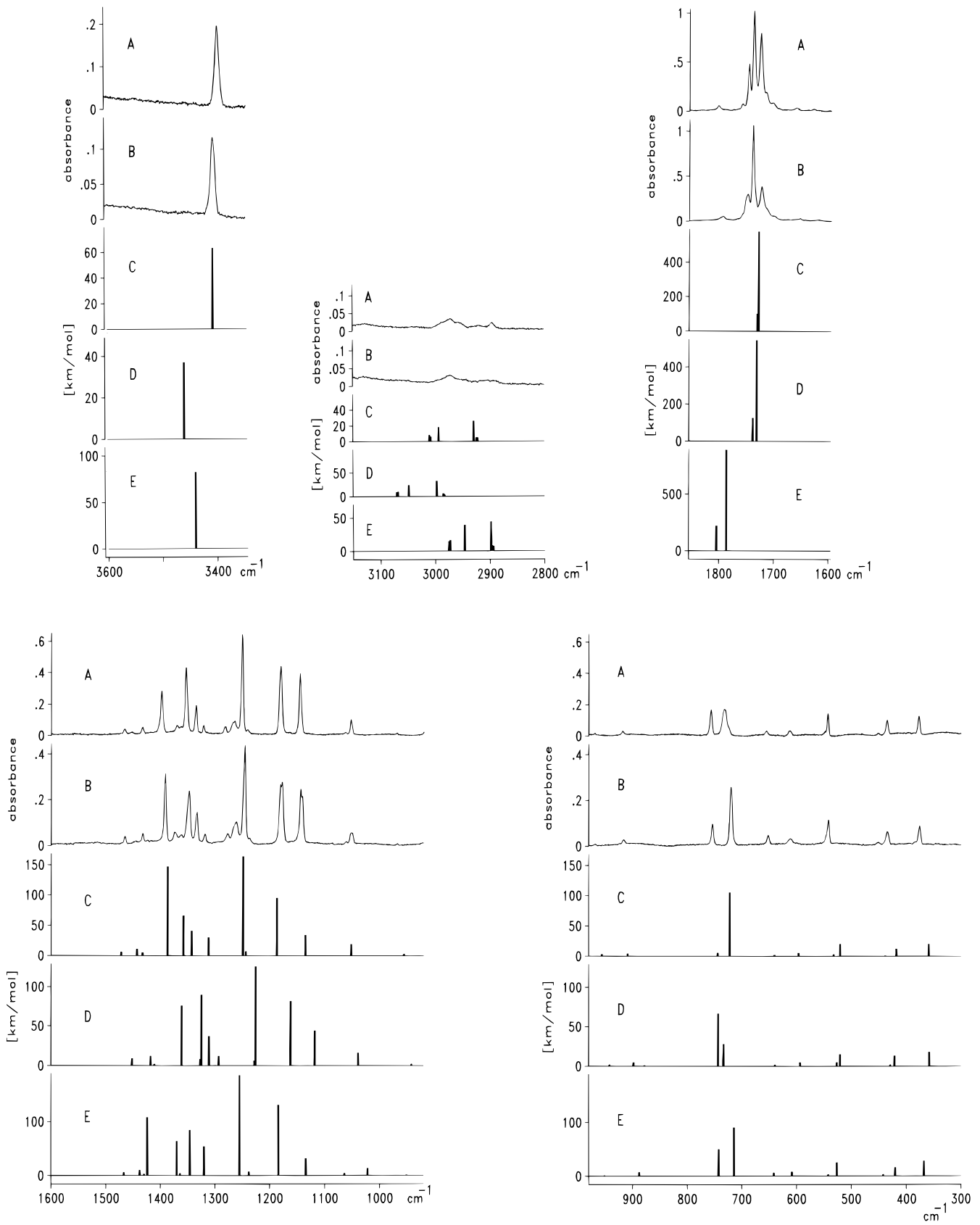

Figure 1. Comparison of the experimental IR spectra of glutarimide isolated in nitrogen (A) and argon (B) matrices, with the spectra predicted theoretically at the MP2/D95V** (C), DFT(BP86)/D95V** (D), and HF/D95V** (E) levels.

experimental and calculated (HF, DFT, and MP2) frequencies and infrared intensities are listed in Table 3. Mode description (vibrational assignment) given in this table is based on potential energy distribution obtained at the MP2 level, except for the modes Q_{28} and Q_{29}, which are better described with PED calculated at the HF level (as will be shown later). It should be emphasized that these three theoretical methods yielded very similar PED values for all corresponding normal modes but these two. Different PEDs have been indicated in the footnotes of Table 3. The overall agreement between the experimental and

TABLE 3: Experimental Wavenumbers ($\tilde{\nu}$, cm^{-1}) and Integral Intensities (I) of Infrared Bands of Glutarimide in Ar and N_2 Matrixes Compared with the Theoretical Harmonic Frequencies ($\tilde{\omega}$, cm^{-1}) and Infrared Intensities (A, km/mol). Theoretical Results Are Calculated with ab Initio HF, Density Functional Theory (BP86 Functional), and MP2 Methods. Vibrational Assignment Is Based on the Calculated Potential Energy Distribution (PED)

mode		experimental				calculated						
		Ar		N_2		HF/D95V**		BP86/D95V**		MP2/D95V**		
no.	sym	$\tilde{\nu}$	I[l]	$\tilde{\nu}$	I[l]	$\tilde{\omega}$[b]	A	$\tilde{\omega}$	A	$\tilde{\omega}$[c]	A	assignment PED[d] (%)
Q_1	A′	3406	59	3397	80	3440	82	3460	37	3407	63	ν(NH) (100)
Q_2	A′	2973[j]				2975	14	3070	9	3010	8	$\nu_1^s CH_2$ (76), $\nu_2^s CH_2$ (18); (C_y)[k]
Q_3	A″					2974	16	3068	10	3009	6	$\nu_1^a CH_2$ (83), $\nu_2^a CH_2$ (17); (C_y)[a]
Q_4	A′					2946	39	3048	24	2993	18	$\nu^a CH_2$ (91); (C_z)
Q_5	A′	2925[j]				2898	44	2997	33	2929	26	$\nu^s CH_2$ (94); (C_z)
Q_6	A″					2896	8	2985	6	2924	5	$\nu_2^a CH_2$ (83), $\nu_1^a CH_2$ (17); (C_y)
Q_7	A′	2902[j]				2894	7	2983	4	2922	5	$\nu_2^s CH_2$ (79),ν_1^s CH_2 (15); (C_y)
		1792	26	1802	14							*e*
				1759								*e*
Q_8	A′	1748		1746		1804	220	1738	125	1730	101	$\nu^s(C_xO)$ (86)
Q_9	A″	1739	710	1737	723	1786	890	1731	547	1729	577	$\nu^a(C_xO)$ (77)
		1723		1725								*e*
		1712		1714								*e*
		1700		1702								*e*
		1652	8	1659	8							*e*
		1619	5	1627	3							*e*
Q_{10}	A′	1465	6	1465	6	1467	6	1452	9	1472	6	sciss CH_2 (98); (C_z)
Q_{11}	A′	1432	6	1433	8	1438	10	1418	12	1443	11	sciss[s] CH_2 (98); (C_y)
Q_{12}	A″	1423[j]				1430	3	1411	2	1433	5	sciss[a] CH_2 (100); (C_y)
Q_{13}	A″	1392	74	1398	65	1424	108	1361	76	1387	147	β(NH) (48), $\nu^a(C_xN)$ (32), ν^a (C_xO) (11)
Q_{14}	A″	1374		1370		1364	4	1327	8	1357	1	wag CH_2 (58) (C_z), $\nu^a(C_yC_z)$ (11)
		1362		1363								*e*
Q_{15}	A′	1348	115	1354	102	1370	64	1325	90	1358	66	$\nu^s(C_xC_y)$ (25), wag[s] CH_2 (24), $\nu^s(C_xN)$ (19), $\beta^s(C_xO)$ (11)
Q_{16}	A″	1334	38	1335	39	1346	84	1311	37	1343	41	wag[a] CH_2 (36), twist CH_2 (28) (C_z), $\nu^a(C_xC_y)$ (13)
Q_{17}	A′	1318	11	1321	12	1320	54	1293	12	1312	30	wag[s] CH_2(52), $\nu^s(C_xN)$ (16), $_\beta{}^s(C_xO)$ (14)
		1277	7	1282	9							*e*
		1262	29	1265	19							*e*
Q_{18}	A″	1246	109	1251	117	1255	186	1226	126	1249	164	wag[a] CH_2 (32), $\nu^a(C_xN)$ (21), β(NH) (20)
Q_{19}	A′	*f*		1241		1238	7	1228	6	1244	7	twist[s] CH_2 (72); (C_y)
Q_{20}	A″	1181	118[i]	1181	116	1184	131	1162	82	1187	95	twist CH_2 (45); (C_z), $\nu^a(C_yC_z)$ (25), $\nu^a(C_xN)$ (11)
		1178										
Q_{21}	A″	1144	90[i]	1145	86	1134	32	1118	44	1135	34	twist[a] CH_2 (64); (C_y)
		1141										
Q_{22}	A′	1061		1063		1064	4	1034	0	1058	0	rock[s] CH_2 (41), rock CH_2 (24); (C_z), $\gamma^s(C_xO)$ (12), twist[s] CH_2 (10)
Q_{23}	A″	1051	20	1053	18	1022	13	1039	16	1052	19	$\nu^a(C_yC_z)$ (49), wag[a] CH_2 (20), wag CH_2 (14); (C_z)
Q_{24}	A′	968	2	969	1	951	1	942	2	956	3	$\beta(R_1)$ (45), rock CH_2 (25); (C_z), rock[s] CH_2 (11); (C_y)
Q_{25}	A′	916	4	918	5	888	7	898	5	909	4	$\nu^s(C_yC_z)$ (64), rock[s] CH_2 (10); (C_y)
Q_{26}	A″					890	0	878	1	890	0	$\nu^a(C_xC_y)$ (39), $\nu^a(C_xN)$ (17), $_\beta{}^a(C_xO)$ (13), rock[a] CH_2 (11)
Q_{27}	A″	858[j]				855	0	840	0	852	0	rock[a] CH_2 (53), $\gamma^a(C_xO)$ (19)
Q_{28}	A′	754	21	757	34	742	50	743	67	744	5	rock CH_2 (27), $\gamma^s(C_xO)$(27), $\nu^s(C_xC_y)$ (23), γNH (18)[g]
Q_{29}	A′	720	78	732	75	714	90	733	28	722	105	γ NH (71), $\nu^s(C_xC_y)$ (16)[h]
Q_{30}	A′	652	10	655	5	641	6	639	2	640	2	β (R_1) (23), $\gamma^s(C_xO)$ (17), $\nu^s(C_xC_y)$ (15), $\nu^s(C_xN)$ (12)
Q_{31}	A″	611	8	613	9	608	8	593	5	596	5	γ^a (C_xO) (67), rock[a] CH_2 (20)
Q_{32}	A′					542	3	526	5	532	3	$\gamma^s(C_xO)$ (31), $\beta(R_2)$ (18), rock[s] CH_2 (16), $\beta(R_1)$ (11)
Q_{33}	A″	541	27	543	27	526	25	520	15	520	20	$\beta^a(C_xO)$ (76), $\nu^a(C_xC_y)$ (17)
Q_{34}	A′	451	3	451	2	442	3	429	2	438	1	$\beta(R_2)$ (35), $\nu^s(C_xN)$ (17), $\beta^s(C_xO)$ (16), rock[s] CH_2 (13)
Q_{35}	A″	435	18	435	20	420	16	421	13	418	12	$\beta(R_3)$ (78)
Q_{36}	A′	376	22	378	20	368	28	358	18	359	20	$\beta^s(C_xO)$ (53), $\beta(R_2)$ (30)
Q_{37}	A′	263[j]				239	2	238	1	250	2	$\tau(R_2)$ (63), $\tau(R_1)$ (28)
Q_{38}	A′					118	6	124	6	116	4	$\tau(R_1)$ (55), $\tau(R_2)$ (45)
Q_{39}	A″					94	0	112	0	94	0	$\tau(R_3)$ (100)

[a] Antisymmetric. [b] HF frequencies scaled by 0.9. [c] MP2 frequencies scaled by 0.96 except for the modes Q_1-Q_7, which are scaled by 0.935. [d] PEDs from MP2 calculations except for modes Q_{28} and Q_{29}; elements lower than 10% are not included. [e] Combinations or overtones, see the text for discussion. [f] Overlapped bands. [g] Different PED values for MP2 $\nu^s(C_xC_y)$ (40) + rock CH_2 (28), and for DFT γNH (46) + $\gamma^s(C_xO)$ (27) + rock CH_2 (15). [h] Different PED values for MP2 γ(NH) (68) + $\gamma^s(C_xO)$ (14), and for DFT γNH (53) + $\nu^s(C_xC_y)$ (25). [i] Matrix effect. [j] Raman data for solid glutarimide taken from ref 47. [k] Symmetric. [l] I, integral absorbances of absorption bands normalized in such a way that the observed intensity sum of all bands is equal to the calculated, at the MP2 level, intensity sum of the corresponding modes.

calculated spectra is very good, particularly at the MP2 level of theory. The calculated infrared intensities of normal modes were extremely helpful in the reliable assignment of the infrared spectrum of glutarimide.

N−H Vibrations. The N−H stretching mode of the monomer glutarimide is readily assigned to a distinct infrared band observed at 3406 cm^{-1} in argon and 3397 cm^{-1} in nitrogen matrices.

It is interesting to note in the infrared spectra of matrix-isolated pyrimidine bases that the corresponding $\nu(N_3H)$ band has been found at very similar wavenumbers: 3430 cm^{-1} (Ar) and 3416 cm^{-1} (N_2) in 1-methyluracil;[24] 3435 cm^{-1} (Ar) in uracil;[36,37] and 3434 cm^{-1} (Ar) in thymine.[36]

The strong absorption at 1392 cm^{-1} in the spectrum of glutarimide in the Ar matrix has been assigned to the NH in-plane bending β(NH) vibration. In a nitrogen matrix, this band

is shifted by 6 cm^{-1} toward higher wavenumbers. Such a shift is typical for β(NH) bands. From the PED shown in Table 3, it is apparent that the corresponding normal mode (Q_{13}) has mainly "NH-bend" character due to the predominant contribution (48%) from the β(NH) internal coordinate, although a significant mixing with the C−N symmetric stretching vibration (32%) is also noted. It is remarkable that the frequency of this mode is so close to that of the corresponding mode, at 1399 and 1395 cm^{-1}, in the infrared spectra of uracil and thymine, respectively.[36]

As can be seen from Table 3, the β(NH) vibration in glutarimide contributes also to the mode Q_{18}, assigned to the very strong infrared band at 1246 cm^{-1} in Ar (1251 cm^{-1} in N_2 matrix). According to the calculated PED, this band can be considered as an analogue of the "amide III band" which occurs around 1250 cm^{-1} in the spectra of amides and peptides.[40]

The NH out-of-plane bending vibration is particularly sensitive to the environment and susceptible to matrix effects, which may account for the differences in wavenumbers of the corresponding infrared band in low-temperature gas matrices.[35−37] It is also expected that this band will be markedly shifted in the spectra of the hydrogen-bonded systems. Thus, a definite assignment of this vibration is very important for the investigation of intermolecular interactions. In the infrared spectrum of glutarimide in an Ar matrix a strong band is observed at 720 cm^{-1}. In a nitrogen matrix this band is considerably blue-shifted (by 12 cm^{-1}) and broadened, which indicates that it is associated with the NH out-of-plane γ(NH) vibration. The frequency of the corresponding mode Q_{29} is very well predicted with three theoretical methods, which confirms our assignment. It follows from PED obtained for Q_{29} that the γ(NH) vibration predominates in this mode; however the calculated contribution from other vibrations is different at each theory level. Furthermore, some discrepancies in PEDs have also been noted for the nearby Q_{28} mode. The relative infrared intensities of these two bands predicted with theoretical methods differ significantly from each other (see Figure 1 C,D,E). The MP2-calculated infrared intensity of the Q_{28} mode is seriously underestimated, whereas that of Q_{29} is overestimated with respect to the experiment.

It is worth noting that infrared intensities calculated at the MP2 level are usually more accurate than those calculated with the HF method using the same basis set.[24,34−35,41−43] However, in our recent MP2/6-31G** calculations we have already encountered a similar problem, since this level of theory failed to predict frequencies and intensities of two normal modes of phenol.[43]

The relative intensities of modes Q_{28} and Q_{29} obtained with the DFT method (BP86 energy functional) are also incorrect since they are just opposite those of the experiment, as is shown in Table 3. The results obtained for these modes at the Hartree−Fock level are in much better agreement with the experiment, although the calculated intensity of Q_{28} is overestimated. It is evident from Table 3 that these discrepancies are related with the different PEDs, calculated at the three theory levels, for Q_{28} and Q_{29}. The plausible explanation of these discrepancies is that calculated infrared intensities depend on the forms of normal modes (which are represented by PED values). Different contributions of internal coordinates within these normal coordinates may sum up or nearly cancel the infrared intensity of the corresponding modes. It seems that PEDs for Q_{28} and Q_{29} calculated with the Hartree−Fock method best describe the nature of these modes; therefore the HF values have been used for assignment of the corresponding two infrared bands. However, it should be emphasized that the best overall agreement between the observed and calculated frequencies and infrared intensities of all other modes of glutarimide has been obtained at the MP2/D95V** level.

It should be noted that the corresponding γ(NH) band occurs at much lower frequencies in the infrared spectra of pyrimidine bases in an Ar matrix: 662 and 659 cm^{-1} for uracil[36] and 1-methyluracil,[24] respectively. This is due to the fact that this band arises from almost "pure" NH out-of-plane vibration in these bases.

C═O Vibrations. Infrared spectra of monomeric glutarimide exhibit a very complex pattern in the region 1800−1600 cm^{-1}, where only two carbonyl stretching modes, ν(C═O), are expected. It is interesting to note that similar complicated structures of the absorption bands arising from C═O stretching vibrations have been observed in the infrared spectra of matrix-isolated uracil, thymine, and its methyl derivatives.[16,24,36−37,44−46] It seems that such a splitting of bands in this frequency region is characteristic of the infrared spectra of all cyclic imides containing two polar C═O groups in the cis position.

It has been concluded that the fundamental transitions corresponding to the stretching motion of these two dipoles enter into strong and multiple Fermi resonances with several overtones and combinations of similar frequencies. The possible combination bands for glutarimide in this frequency range are 1432 + 376 = 1808; 1348 + 451 = 1799; 1181 + 611 = 1792; 1246 + 541 = 1787; 1061 + 720 = 1781; 1392 + 376 = 1768; 1348 + 376 = 1724; 1181 + 541 = 1722; 968 + 754 = 1722; 1061 + 652 = 1713; 1334 + 376 = 1710; 1051 + 652 = 1703; 916 + 720 = 1636; 1246 + 376 = 1622 cm^{-1} (in an Ar matrix).

According to our calculations, the symmetric and antisymmetric C═O stretching vibrations of two equivalent carbonyl groups in glutarimide have very similar energy. The frequency of the former is only slightly higher than that of the latter. However, the predicted infrared intensities of these two C═O stretching modes are very different; the antisymmetric vibration generates the infrared band which is 4−5 times more intense than the symmetric counterpart. It should be emphasized that the theoretical results are consistent regardless of the method applied.

The predicted frequencies and the intensity pattern of ν(C═O) absorptions have proved to be of great help in assigning the spectra. In both matrices, the band of the highest intensity, located at 1739 cm^{-1} in Ar and 1737 cm^{-1} in N_2, is undoubtedly associated with the antisymmetric C═O stretching vibration (Q_9 mode). The higher wavenumber band, observed at 1748 cm^{-1} in an Ar matrix (1746 cm^{-1} in N_2), has been attributed to the symmetric C═O stretching vibration (Q_8). A third band in this cluster, observed at 1723 cm^{-1} (Ar) and 1725 cm^{-1} (N_2), corresponds to some combination tone (as indicated above) which borrows infrared intensity from one of the ν(CO) fundamentals through the Fermi resonance mechanism. It should be noted that both the MP2 method and BP86 functional predicted well both the frequencies and infrared intensities of these two modes, whereas the HF method overestimated these values. The corresponding C═O stretching bands in matrix-isolated infrared spectra of pyrimidine bases have been found at very similar wavenumbers.[24,36,37]

The CO in-plane bending vibrations have been assigned to medium-intensity infrared bands at 536 and 391 cm^{-1} in the spectrum of uracil[36,37] and at 538 and 389 cm^{-1} in 1-methyluracil.[24] It is interesting to note that the corresponding antisymmetric and symmetric CO in-plane bending vibrations in glutarimide give rise to the medium-intensity bands at almost identical wavenumbers, 541 cm^{-1} (Q_{33}) and 376 cm^{-1} (Q_{36}), respectively. Although the calculated frequency of the former is consistently underestimated (by about 15−20 cm^{-1}), at all

theory levels, the predicted infrared intensities of these modes are in very good agreement with experimental values.

According to PED, the CO out-of-plane bending vibrations, γ(CO), in glutarimide are strongly mixed with ring vibrations and CH_2 deformations; therefore they are not observed as characteristic bands, but contribute to several bands in the range from 860 to about 500 cm^{-1}. The very weak infrared band at 611 cm^{-1} corresponds to the mode Q_{31}, which contains a significant contribution from the antisymmetric γ(CO). The symmetric γ(CO) vibration contributes to the mode Q_{32}, but the corresponding band is too weak to be observed in the experimental spectrum. It seems that the extensive coupling of γ(CO) with other vibrations is the likely reason for the anomalously low intensities of the "γ(CO) bands" in the infrared spectrum of glutarimide.

It should be noted that in 1-methyluracil the corresponding γ(CO) modes have significantly higher infrared intensities and also higher frequencies, 802 and 761 cm^{-1}.[24] This can be attributed to a different coupling of these vibrations in 1-methyluracil.

CH_2 and Ring Vibrations. The C−H stretching region in the infrared spectra of cyclic amides and alkanes is noted for being strongly affected by anharmonic resonances.[40] In glutarimide Fermi resonances may occur between the C−H stretching fundamentals and overtones of CH_2 deformation modes as well as combinations involving the NH bending or CH bending and C═O stretching vibrations, similarly as in substituted amides. It can be seen from Figure 1 that several weak absorptions appear in the region between 3000 and 2850 cm^{-1}, both in argon and nitrogen matrices. Such a low intensity of the bands due to C−H stretching modes seems to be typical for infrared spectra of monomeric heterocycles isolated in low-temperature matrices.[24,36,37] Therefore, the C−H stretching vibrations of glutarimide have been assigned from the Raman spectrum of crystalline glutarimide,[47] where these modes generate two very intense bands, at 2973 and 2902 cm^{-1}, and a shoulder at 2925 cm^{-1}. It should be noted that the calculated (and scaled) HF and MP2 frequencies of these modes are quite close to the experimental values, as shown in Table 3. In the assignment of the C−H stretching modes we were guided by the fact that in compounds where the CH_2 group is attached to a carbonyl group the corresponding symmetric CH_2 stretching vibration is observed as a strong Raman band around 2910 cm^{-1}.[40,48] Thus, it has been concluded that a very strong band at 2902 cm^{-1} in the Raman spectrum of glutarimide corresponds to stretching vibrations in the C_yHH groups, adjacent to C_x═O (Q_6 and Q_7 modes). These two modes have almost identical frequencies, as revealed by calculations; therefore they may give rise to only one band observed in the spectrum. The next strong band at 2973 cm^{-1} in the Raman spectrum may result from an overlap of three modes, Q_2, Q_3, and Q_4, since their frequencies, predicted at the MP2 level, are very similar. A shoulder at 2925 cm^{-1} has been assigned to the stretching vibration (Q_5) in the C_zHH group, which is supported by the presence of a similar band in the spectrum of cyclohexane.[49]

The methylene scissoring vibrations (sciss CH_2) in glutarimide have been assigned by comparison with the spectra of related compounds. In cyclohexane, these modes generate weak absorptions in the range 1475−1450 cm^{-1}.[49] Bellamy[40] has noted for the compounds containing the methylene group adjacent to a carbonyl group that the position of this band is shifted to lower wavenumbers (1425−1400 cm^{-1}) while its infrared intensity increases. A similar effect has also been observed in the matrix-isolated infrared spectrum of glutarimide, and it was confirmed in our calculations. As can be seen from Table 3, the calculated frequencies of Q_{11} and Q_{12} are lower that that of the mode Q_{10}. The two former correspond to the methylene scissoring vibrations in the C_yHH groups (attached to C_x═O), whereas the latter arises from the scissoring vibration in the C_zHH group. It seems that these characteristic bands corresponding to stretching and scissoring vibrations of different methylene groups in glutarimide can be used as the diagnostic bands in other spectroscopic studies on larger molecules (e.g. steroids) containing methylene groups in various environments.

The remaining CH_2 deformation modes, wagging, twisting, and rocking vibrations, appear to be strongly coupled with different ring vibrations in glutarimide. According to PED, the CH_2 wagging modes have a large contribution to several bands observed in the range 1374−1050 cm^{-1}, as shown in Table 3. The very strong band at 1348 cm^{-1} (Ar) has been assigned to the mode Q_{15}, which corresponds to the "ring breathing vibration" coupled with the CH_2 wagging vibrations. This is supported by a similar assignment of the strong, characteristic band observed at about 1360 cm^{-1} in the infrared spectra of antineoplaston A10, the new antitumor drug containing glutarimide.[48,50] We, therefore, suggest that this infrared band can also be used as the "marker band ", for the presence of the glutarimide ring in large molecular systems. The next strong band at 1246 cm^{-1} in the infrared spectrum of glutarimide in an Ar matrix (assigned to Q_{18}) corresponds to the "amide III band", as discussed earlier.

An assignment of the remaining bands in the range 1374−1262 cm^{-1} is quite difficult since these bands are weak, broad, and closely spaced. Bands at 1374, 1334, and 1318 cm^{-1} have been assigned to the fundamentals Q_{14}, Q_{16}, and Q_{17}, respectively, since they correspond to bands of similar wavenumbers in the spectra of related compounds.[40,49] A doublet observed at 1277/1262 cm^{-1} in Ar, which is slightly shifted in a N_2 matrix, originates, most probably, from combination tones (for example, 611 + 652 = 1263 and 541 + 72 0 = 1261 in Ar) which borrow their intensity via anharmonic resonances with the nearby Q_{18} fundamental mode of the same symmetry. Similarly, a weak band at 1362 cm^{-1} may arise from Fermi resonance between the combination (611 + 754 = 1365 cm^{-1}) with the fundamental Q_{14} at 1374 cm^{-1}. The methylene twisting vibrations (Q_{20} and Q_{21}) have been assigned to the strong infrared bands observed at 1181 and 1141 cm^{-1}. Band splitting observed for these modes in an argon matrix disappears in a nitrogen matrix; therefore, it is ascribed to a matrix effect. As follows from calculations, the third CH_2 twisting vibration (Q_{19}) in glutarimide generates a band of very low infrared intensity. Furthermore, its frequency is very similar to that of the Q_{18} mode; therefore it is probably hidden under the strong Q_{18} absorption. Theoretical data indicate that the CH_2 rocking vibrations are extensively coupled with the ring deformation modes and contribute to extremely weak infrared bands in the range 1060−850 cm^{-1} and also to several bands in the low-frequency region.

The frequencies of ring deformations Q_{34}, Q_{35}, and Q_{36} are quite well predicted by theory. As is seen in Table 2, a high level of conformity between the BP86/D95V** and MP2/D95V** results is observed in the range below 640 cm^{-1}. The remaining three modes, Q_{37}, Q_{38}, and Q_{39}, corresponding to torsion vibrations, were below the range covered by the matrix experiment. The predicted frequencies of these modes are in the range 250−90 cm^{-1}. A band observed at 263 cm^{-1} in the Raman spectrum of solid glutarimide, which was asssigned to the ring torsion vibration,[47] corresponds very well to the frequency of 250 cm^{-1}, calculated at the MP2/D95V** level. It should be mentioned that for uracils[24,36] torsion vibrations of the ring contribute to the normal modes of higher frequencies.

For 2(1*H*)-pyrimidinone[35a] or 4(3*H*)-pyrimidinone[35b] torsional modes give rise to infrared bands near 700 cm^{-1}. The very low frequencies of the torsion vibrations of glutarimide correspond to a greater flexibility of the glutarimide ring when compared to the above-mentioned compounds.

Conclusions

The important conclusions from the present study can be summarized as follows.

1. A good agreement between the calculated (HF, MP2, and DFT/BP86) and experimental infrared intensities and frequencies of glutarimide confirms the reliability of the presented vibrational band assignment.

2. The best overall agreement between the calculated and experimental spectra has been obtained at the MP2/D95V** level, although for some modes, the infrared intensities predicted by HF or DFT methods agreed better with experiment.

3. The HF frequencies (after scaling) are overestimated for most modes, in particular, for C═O stretching vibrations, whereas frequencies calculated at the BP86/D95V** level are closer to MP2 and experimental results.

4. The bond distances predicted with the DFT method (the BP86 functional) are too long, while the frequencies of C═O stretchings and other modes are very well reproduced. This effect can be attributed to some error cancellation.

5. A striking similarity is noted for frequencies of the corresponding CO and NH vibrations in glutarimide and in uracil, thymine, and their methyl derivatives.

6. The significant flattening of the glutarimide ring, predicted by calculations, indicates its structural resemblance to pyrimidine bases.

7. It is suggested that some glutarimide drugs are able to intercalate between nucleic base pairs in the DNA helix, or they may act as an antagonist of uracil and thymine in biological processes. This may interfere with nucleic acid or protein synthesis in cells. These conclusions are in accordance with previous experimental results indicating that some glutarimide drugs may interact with DNA.

Acknowledgment. This work was supported in part by the ECC research project S&T Cooperation with Central and Eastern European Countries ERB CIPA-CT 93-0108 and by the Technical University of Wrocław under Grants Nos. 341-589 and 341-695. The authors would like to thank the Poznań Supercomputing and Networking Center for a generous computer time grant.

References and Notes

(1) Rahman, A.; Luc, P.-V. T.; Schein, P. S.; Woolley, P. V. *Cancer Res.* **1984**, *44*, 149.

(2) (a) Harris, A. I. *Drugs Today* **1984**, *20*, 167. (b) Gale, K. E.; Andersen, J. W.; Tormey, D. C.; Mansour, E. G.; Davis, T. E.; Horton, J.; Wolter, J. M.; Smith, T. J.; Cummings, F. J. *Cancer* **1994**, *73*, 354.

(3) (a) Burzynski, S. R. *Adv. Exp. Clin. Chemother.* **1988**, *6*, 45. (b) Burzynski, S. R.; Hai, T. T. *Drugs Fut.* **1985**, *10*, 103.

(4) (a) Tsuda, H.; Sugihara, S.; Nishida, H.; Hara, H.; Eriguchi, N.; Ishii, K.; Sasaki, K.; Yoshimura, S.; Tanaka, N. *Jpn. J. Cancer Res.* **1992**, *83*, 527. (b) Yoshida, H.; Nishida, H.; Kitsuu, T.; Fukushima, K.; Eriguchi, N.; Hara, H.; Nakayama, T.; Ohishi, K.; Tsuda, H. *J. Jpn. Soc. Cancer Ther.* **1992**, *27*, 1943.

(5) (a) Lehner, A. F.; Burzynski, S. R.; Hendry, L. B. *Drugs Exp. Clin. Res.* **1986**, *12* (Suppl. 1), 57. (b) Hendry, L. B.; Muldoon, T. G.; Burzynski, S. R.; Copland, J. A.; Lehner, A. F. *Drugs Exp. Clin. Res.* **1987**, *13* (Suppl. 1) 77. (b) Hendry, L. B.; Muldoon, T. G. *J. Steroid Biochem.* **1988**, *30*, 325.

(6) Eriguchi, N.; Hara, H.; Yoshida, H.; Nishida, H.; Nakayama, T.; Ohishi, K.; Tsuda, H.; Ikeda, I. *J. Jpn. Soc. Cancer Ther.* **1988**, *23*, 1560.

(7) Otani, T.; Minami, Y.; Matsumoto, H.; Marunaka, T.; Lou, Z.-X.; Yu, Q.-W. *J. Antibiot.* **1989**, *42*, 654.

(8) Sugawara, K.; Nishiyama, Y.; Toda, S.; Komiyama, N.; Hatori, M.; Moriyama, T.; Sawada, Y.; Kamei, H.; Konishi, M.; Oki, T. *J. Antibiot.* **1992**, *45*, 1433.

(9) (a) Sonoda, T.; Osada, H.; Uzawa, J.; Isono, K. *J. Antibiot.* **1991**, *44*, 160. (b) Sonoda, T.; Kobayashi, K.; Ubukata, M.; Osada, H.; Isono, K. *J. Antibiot.* **1992**, *45*, 1963.

(10) Carrasco, L.; Jimenez, A.; Vazquez, D. *Eur. J. Biochem.* **1976**, *64*, 1.

(11) Bottger, E. C.; Blanar, M. A.; Flavell, R. A. *Immunogenetics* **1988**, *28*, 215.

(12) Shull, G. E. *J. Theor. Biol.* **1984**, *110*, 461.

(13) Grollman, A. P. *Biochemistry* **1966**, *56*, 1867.

(14) Xu, S.; Clark, L. B. *J. Am. Chem. Soc.* **1994**, *116*, 9227.

(15) Thompson, J. W., Jr.; Leroi, G. E.; Popov, A. I. *Spectrochim. Acta* **1975**, *31*, 1553.

(16) Szczesniak, M.; Nowak, M. J.; Rostkowska, H.; Szczepaniak, K.; Person, W. B.; Shugar, D. *J. Am. Chem. Soc.* **1983**, *105*, 5969.

(17) Frisch, M. J.; Trucks, G. W.; Schlegel, H. B.; Gill, P. M. W.; Johnson, B. G.; Robs, M. A.; Cheeseman, J. R.; Keith, T.; Petersson, J. A.; Mongomery, K.; Raghavachari, K.; Al.-Laham, M. A.; Zakrzewski, V. G.; Ortiz, J. V.; Foresman, J. B.; Peng, C. Y.; Ayala, P. Y.; Chen, W.; Wong, M. W.; Andres, J. L.; Replogle, E. S.; Gomperts, R.; Martin, R. L.; Fox, D. J.; Binkley, J. S.; DeFrees, D. J.; Baker, J.; Stewart, J. P.; Head-Gordon, M.; Gonzales, C.; Pople, J. A. *Gaussian 94, Revision B.3*; Gaussian, Inc.: Pittsburgh, 1995.

(18) Møller, C.; Plesset, M. S. *Phys. Rev.* **1934**, *46*, 618.

(19) Parr, R. G.; Yang, W. *Density Functional Theory of Atoms and Molecules*; Oxford University Press: Oxford, 1989.

(20) Huzinaga, S. *J. Chem. Phys.* **1965**, *42*, 1293.

(21) Dunning, T. H.; Hay, P. J. In *Modern Theoretical Chemistry;* Schaefer, H. F., III, Ed.; Plenum Press: New York, 1976; Vol. 3, p 1.

(22) Hariharan P. C.; Pople, J. A. *Theor. Chim. Acta* **1973**, *28*, 213.

(23) Szostak, M. M.; Misiaszek, T.; Roszak, S.; Rankin, J. G.; Czernuszewicz, R. S. *J. Phys. Chem.* **1995**, *99*, 14992.

(24) Nowak, M. J.; Lapinski, L.; Bieńko, D. C.; Michalska, D. *Spectrochim. Acta* **1997**, *53A*, 856.

(25) Becke, A. D. *Phys. Rev. A* **1988**, *38*, 3098.

(26) Perdew, J. P. *Phys. Rev. B* **1986**, *33*, 8822.

(27) Lee, C.; Yang, W.; Parr, R. G. *Phys. Rev. B* **1988**, *37*, 785.

(28) Becke, A. D. *J. Chem. Phys.* **1993**, *98*, 5648.

(29) Kohn, W.; Sham, L. J. *Phys. Rev.* **1965**, *140*, 1133.

(30) Fogarasi, G,; Pulay, P. In *Vibrational Spectra and Structure;* Durig, J. R., Ed.; Elsevier: New York, 1985; Vol 13.

(31) Schachtschneider, J. H. Vibrational Analysis of Polyatomic Molecules. Technical Report Nos. 231−64 and 57−65, Shell Development Co., Emeryville, CA, 1970.

(32) Califano, S. *Vibrational States*; Wiley: New York, 1976.

(33) (a) Morino, Y.; Kuchitsu, J. *J. Chem. Phys.* **1952**, *20*, 1809. (b) Keresztury, G.; Jalsovszky, G. *J. Mol. Struct.* **1971**, *10*, 304.

(34) Kwiatkowski, J. S.; Leszczyński, J. *J. Mol. Struct. (THEOCHEM)* **1994**, *312*, 201.

(35) (a) Lapinski, L.; Nowak, M. J.; Leś, A.; Adamowicz, L. *Vib. Spectrosc.* **1995**, *8*, 331. (b) Nowak, M. J.; Lapinski, L.; Fulara, J. Leś, A.; Adamowicz, L. *J. Phys. Chem.* **1992**, *96*, 1562.

(36) Leś, A.; Adamowicz, L.; Nowak, M. J.; Lapinski, L. *Spectrochim. Acta* **1992**, *48A*, 1385.

(37) Barnes, A. J.; Stuckey, M. A.; Le Gall L. *Spectrochim. Acta* **1984**, *40A*, 419.

(38) Petersen, C. S. *Acta Chem. Scand.* **1971**, *25*, 379.

(39) Michalska, D.; Morzyk, B.; Wojciechowski, W.; Głowiak, T. *Inorg. Chim. Acta* **1995**, *248*, 159.

(40) Bellamy, L. J. *The Infrared Spectra of Complex Molecules*, Chapman and Hall Press: London, 1975; Chapters 2, 5, and 12.

(41) Hess, B. A., Jr.; Allen, W. D.; Michalska, D.; Schaad, L. J.; Schaefer H. F., III. *J. Am. Chem. Soc.* **1987**, *109*, 1615.

(42) Michalska, D.; Chojnacki, H.; Hess, B. A., Jr.; Schaad, L. J. *Chem. Phys. Lett.* **1987**, *141*, 376.

(43) Michalska, D.; Bieńko, D. C.; Abkowicz-Bieńko, A. J.; Latajka, Z. *J. Phys. Chem.* **1996**, *100*, 17786.

(44) Szczesniak, M.; Nowak, M. J.; Szczepaniak, K.; Chin, S.; Scott, I.; Person, W. B. *Spectrochim. Acta* **1985**, *41A*, 223.

(45) Szczesniak, M.; Nowak, M. J.; Szczepaniak, K.; Person, W. B. *Spectrochim. Acta* **1985**, *41A*, 237.

(46) Wojcik, M. J.; Rostkowska, H.; Szczepaniak, K.; Person, W. B. *Spectrochim. Acta* **1989**, *45A*, 499.

(47) Morzyk, B. Ph.D. Thesis, Technical University of Wroclaw, Wroclaw, 1996.

(48) Michalska, D.; *Spectrochim. Acta* **1993**, *49A*, 303.

(49) Wiberg, K. B.; Shrake, A. *Spectrochim. Acta* **1973**, *29A*, 583.

(50) Michalska, D.; *Drugs Exp. Clin. Res.* **1990**, *16*, 343.